JVI Journals.ASM.org

Phosphatidylinositol-(4,5)-Bisphosphate Acyl Chains Differentiate Membrane Binding of HIV-1 Gag from That of the Phospholipase Cδ1 Pleckstrin Homology Domain

Balaji Olety,[a] Sarah L. Veatch,[b] Akira Ono[a]

Department of Microbiology and Immunology, University of Michigan Medical School, Ann Arbor, Michigan, USA[a]; Department of Biophysics, University of Michigan, Ann Arbor, Michigan, USA[b]

ABSTRACT

HIV-1 Gag, which drives virion assembly, interacts with a plasma membrane (PM)-specific phosphoinositide, phosphatidylinositol-(4,5)-bisphosphate [$PI(4,5)P_2$]. While cellular acidic phospholipid-binding proteins/domains, such as the $PI(4,5)P_2$-specific pleckstrin homology domain of phospholipase Cδ1 ($PH_{PLC\delta1}$), mediate headgroup-specific interactions with corresponding phospholipids, the exact nature of the Gag-$PI(4,5)P_2$ interaction remains undetermined. In this study, we used giant unilamellar vesicles (GUVs) to examine how $PI(4,5)P_2$ with unsaturated or saturated acyl chains affect membrane binding of $PH_{PLC\delta_1}$ and Gag. Both unsaturated dioleoyl-$PI(4,5)P_2$ [DO-$PI(4,5)P_2$] and saturated dipalmitoyl-$PI(4,5)P_2$ [DP-$PI(4,5)P_2$] successfully recruited $PH_{PLC\delta_1}$ to membranes of single-phase GUVs. In contrast, DO-$PI(4,5)P_2$ but not DP-$PI(4,5)P_2$ recruited Gag to GUVs, indicating that $PI(4,5)P_2$ acyl chains contribute to stable membrane binding of Gag. GUVs containing $PI(4,5)P_2$, cholesterol, and dipalmitoyl phosphatidylserine separated into two coexisting phases: one was a liquid phase, and the other appeared to be a phosphatidylserine-enriched gel phase. In these vesicles, the liquid phase recruited $PH_{PLC\delta_1}$ regardless of $PI(4,5)P_2$ acyl chains. Likewise, Gag bound to the liquid phase when $PI(4,5)P_2$ had DO-acyl chains. DP-$PI(4,5)P_2$-containing GUVs showed no detectable Gag binding to the liquid phase. Unexpectedly, however, DP-$PI(4,5)P_2$ still promoted recruitment of Gag, but not $PH_{PLC\delta_1}$, to the dipalmitoyl-phosphatidylserine-enriched gel phase of these GUVs. Altogether, these results revealed different roles for $PI(4,5)P_2$ acyl chains in membrane binding of two $PI(4,5)P_2$-binding proteins, Gag and $PH_{PLC\delta_1}$. Notably, we observed that nonmyristylated Gag retains the preference for $PI(4,5)P_2$ containing an unsaturated acyl chain over DP-$PI(4,5)P_2$, suggesting that Gag sensitivity to $PI(4,5)P_2$ acyl chain saturation is determined directly by the matrix-$PI(4,5)P_2$ interaction, rather than indirectly by a myristate-dependent mechanism.

IMPORTANCE

Binding of HIV-1 Gag to the plasma membrane is promoted by its interaction with a plasma membrane-localized phospholipid, $PI(4,5)P_2$. Many cellular proteins are also recruited to the plasma membrane via $PI(4,5)P_2$-interacting domains represented by $PH_{PLC\delta_1}$. However, differences and/or similarities between these host proteins and viral Gag protein in the nature of their $PI(4,5)P_2$ interactions, especially in the context of membrane binding, remain to be determined. Using a novel giant unilamellar vesicle-based system, we found that $PI(4,5)P_2$ with an unsaturated acyl chain recruited $PH_{PLC\delta_1}$ and Gag similarly, whereas $PI(4,5)P_2$ with saturated acyl chains either recruited $PH_{PLC\delta_1}$ but not Gag or sorted these proteins to different phases of vesicles. To our knowledge, this is the first study to show that $PI(4,5)P_2$ acyl chains differentially modulate membrane binding of $PI(4,5)P_2$-binding proteins. Since Gag membrane binding is essential for progeny virion production, the $PI(4,5)P_2$ acyl chain property may serve as a potential target for anti-HIV therapeutic strategies.

A large number of proteins bind to the cytoplasmic surface of cellular membranes via headgroup-dependent interactions with acidic lipids. A prominent example is the interaction between the headgroup of a plasma-membrane (PM)-specific phospholipid, phosphatidylinositol-(4, 5)-bisphosphate [$PI(4,5)P_2$], and the pleckstrin homology (PH) domain of phospholipase Cδ1 ($PH_{PLC\delta_1}$). However, for many cytoplasmic proteins, binding to a specific membrane requires not only a specific interaction with a headgroup of a single lipid species but also depends on other factors, such as membrane curvature or the presence of other molecules (lipids or proteins). These factors can serve as additional layers of regulation to ensure specific targeting to and/or stable retention at a particular membrane or membrane site (1).

During HIV-1 assembly, the viral structural protein Gag, which drives the assembly process, binds to and localizes at the PM to form nascent virus particles. Gag is synthesized as a polyprotein that contains four domains, matrix (MA), capsid (CA), nucleocapsid (NC), and p6, and two spacer peptides, SP1 and SP2. The MA domain at the Gag N terminus is important for proper targeting and membrane binding of Gag, whereas the downstream do-

Received 25 March 2015 Accepted 13 May 2015

Accepted manuscript posted online 20 May 2015

Citation Olety B, Veatch SL, Ono A. 2015. Phosphatidylinositol-(4,5)-bisphosphate acyl chains differentiate membrane binding of HIV-1 Gag from that of the phospholipase Cδ1 pleckstrin homology domain. J Virol 89:7861–7873. doi:10.1128/JVI.00794-15.

Editor: W. I. Sundquist

Address correspondence to Akira Ono, akiraono@umich.edu.

doi:10.1128/JVI.00794-15

mains drive multimerization and release of the nascent virus particles. Gag is cotranslationally modified by N-myristoylation, which is essential for Gag membrane binding. Binding of Gag to the PM and hence efficient virus production are also dependent on cellular $PI(4,5)P_2$ (2), for which the highly basic region (HBR) in MA forms a binding interface (3–5). The interaction of Gag with $PI(4,5)P_2$ depends not only on the overall positive charge of HBR but also on the specific order of lysines and arginines in the HBR (6).

In addition to $PI(4,5)P_2$, the PM contains other lipids that are implicated in Gag membrane binding. Cell-based and *in vitro* studies have shown that cholesterol enhances Gag membrane binding (7–9). One of these studies also showed that liposomes that contain another acidic lipid phosphatidylserine (PS) but lack $PI(4,5)P_2$ can recruit Gag efficiently in a manner dependent on lipid acyl chains (8). A nuclear magnetic resonance (NMR)-based study showed that MA can sequester acyl chains of various phospholipids, including PS (10). Therefore, acyl chains of non-$PI(4,5)P_2$ lipids may play an important role in Gag membrane binding. Phospholipid acyl chains have also been implicated in genome replication and virion infectivity of RNA and DNA viruses (11, 12), suggesting that these components may provide a broad range of targets for antivirals. Notably, while earlier studies suggested that MA also interacts with short acyl chains of water-soluble $PI(4,5)P_2$ (4, 13), the functional significance of $PI(4,5)P_2$ acyl chains in membrane binding of full-length Gag has not been addressed.

MA also interacts with RNA (14–17). RNA bound to MA inhibits binding of Gag to acidic lipid-containing liposomes, such as those composed of palmitoyl-oleoyl-phosphatidylcholine (POPC) and POPS (18–20). Such inhibition is observed with both *in vitro*-synthesized Gag (18–20) and Gag expressed in cells (21). Furthermore, a similar inhibition was recently observed for Gag binding to cell membranes (22). Notably, when $PI(4,5)P_2$ is included in the liposomes, Gag overcomes this inhibition and binds efficiently to the liposomes (18). Furthermore, $PI(4,5)P_2$ or a related molecule is able to outcompete nucleic acids for binding to MA (23–25), suggesting that $PI(4,5)P_2$ can promote RNA displacement. These results collectively support a model in which $PI(4,5)P_2$ displaces RNA from MA HBR or otherwise alters the MA-RNA interaction, while promoting stable Gag membrane binding as a membrane anchor. It is also conceivable that PS, which represents the major fraction of total PM acidic phospholipids, serves as a membrane anchor for Gag once RNA is removed from MA HBR.

In this study, we used giant unilamellar vesicles (GUVs) to address the roles played by acyl chains of $PI(4,5)P_2$ in Gag membrane binding. This experimental system allowed us to study interactions within a membrane that is largely flat and thus mimics the natural membrane curvature encountered by cytoplasmic proteins in cells. Curvature effects could also impact acyl chain dynamics, which have been observed in model systems through two different approaches (26, 27). Also, the use of GUVs, which are easily visualized by fluorescence microscopy, enabled us to probe Gag binding to membranes containing multiple phases of lipids in different physical states. Using this system, we found that $PI(4,5)P_2$ acyl chains differentially affect membrane binding of Gag and $PH_{PLC\delta_1}$, a representative host origin $PI(4,5)P_2$-interacting domain. We observed that $PI(4,5)P_2$ with saturated acyl chains supports binding of $PH_{PLC\delta_1}$ but not Gag in single-phase GUVs. Moreover, in two-phase GUVs that contain liquid and PS-enriched gel phases, $PI(4,5)P_2$ with unsaturated acyl chains recruits both Gag and $PH_{PLC\delta_1}$ to the liquid phase, whereas $PI(4,5)P_2$ with saturated acyl chains directs Gag to the gel phase and $PH_{PLC\delta_1}$ to the liquid phase. Binding of Gag to both phases requires Gag-$PI(4,5)P_2$ interactions. Altogether, these results reveal a complex nature of the role for acyl chains in $PI(4,5)P_2$-dependent Gag membrane binding, which is very distinct from that observed in membrane binding of the canonical $PI(4,5)P_2$-binding domain, $PH_{PLC\delta_1}$.

MATERIALS AND METHODS

Reagents. All lipids were purchased from Avanti Polar Lipids (Alabaster, AL, USA) except for DP-$PI(4,5)P_2$ and DPPS, which were purchased from Echelon Biosciences (Salt Lake City, UT, USA). The far-red fluorescent lipid probe 1,1′-dioctadecyl-3,3,3′,3′-tetramethylindodicarbocyanine,4-chlorobenzenesulfonate salt (DiD) was purchased from Life Technologies (Carlsbad, CA, USA). RNase (RNase A) and RNasin were purchased from Qiagen and Promega, respectively. Fluorescein isothiocyanate (FITC)-labeled poly-L-lysine was purchased from Sigma-Aldrich.

***In vitro* translation of proteins by using wheat germ lysates.** Sequences encoding wild-type (WT) Gag-yellow fluorescent protein (YFP), 1GA Gag-YFP, delNC Gag-YFP, HBR/RKswitch Gag-YFP, and PH-green fluorescent protein (GFP), which were derived from pNL4-3/Gag-YFP (3), pNL4-3/1GA/Gag-YFP (28), pNL4-3/delNC/Gag-YFP (28), and pNL4-3/HBR/RKswitch/Gag-YFP (6) constructs and the original PH-GFP expression plasmid (a kind gift from Tamas Balla), respectively, were cloned into pIVEX1.3WG-BO. A custom multiple-cloning site sequence was introduced into pIVEX1.3WG (5-Prime) to construct pIVEX1.3WG-BO. A coupled *in vitro* transcription and translation reaction was performed using these plasmids and the RTS-100 wheat germ continuous exchange, cell-free kit as recommended by the manufacturer (5-Prime). The total ionic strength of the wheat germ reaction mixtures, which were buffered with 100 mM potassium acetate and 25 mM HEPES, was approximately 150 mM (Mathias Christoph [5-Prime], personal communication) (75 mM upon mixing with GUV suspensions). The pH of the GUV-wheat germ lysate mixtures containing either WT Gag-YFP or PH-GFP was determined to be 7.3. RNasin was included in the reaction mixture unless the effects of RNase treatment were to be analyzed. The reaction was performed for 24 h at 22°C. After the reaction, the lysates containing the translated proteins were subjected to centrifugation at 16,200 × *g* for 15 min to remove aggregated materials, and the supernatants containing the translated proteins were used for the GUV-binding assays.

Preparation of GUVs and GUV-binding assay. Lipids were mixed in glass vials, and the mixture of lipids was spread onto conductive sides of indium-tin oxide (ITO)-coated glass slides on a platform preheated to 65°C, a temperature higher than the melting temperature (T_m) of saturated lipids, such as DPPS used in this study (T_m = 54°C). The lipid-coated glass slides were incubated inside a vacuum chamber for at least 90 min to remove any residual organic solvents. For electroformation, the reaction chamber was constructed as follows. A gasket that is made of polydimethylsiloxane (PDMS; Sylgard 184; Dow Corning) was placed on one of the lipid-coated glass slides and gently pressed to ensure tight attachment. The resulting chamber was then filled with 300 mM sucrose solution that was preheated to 65°C. Another coated glass slide was placed on the filled chamber with the ITO- and lipid-coated side facing the solution. The slide setup was then placed in a 65°C incubator, and an alternating current of 1 V and 10 Hz was applied for 90 min. For an additional 10 min, a reduced frequency of 2 Hz was applied. Following the electroformation, the assembly was left at room temperature for cooling. The PDMS chamber was disassembled, and the sucrose suspension containing GUVs was harvested by using a cut tip and then immediately used for the GUV-binding assay. When DiD (0.05 mol% in epifluorescence experiments and 0.25 mol% in confocal microscopy experiments) was included in the mixture of lipids, the steps described above were performed with minimal

exposure to light. For the GUV-binding assay, a freshly prepared GUV suspension and a wheat germ lysate containing translated proteins were mixed at a 1:1 ratio in an Eppendorf polypropylene tube using a cut tip. When indicated, RNase was added to the mixture of a GUV suspension and a wheat germ lysate at a final concentration of 10 μg/μl at the beginning of the GUV-binding reaction. Subsequently (within 1 min of mixing), the mixture was transferred onto a clean coverslip for image acquisition. Epifluorescence images were acquired using a Nikon TE2000U epifluorescence microscope and a 60× objective lens (Plan APO, 1.40 numerical aperture [NA]; Nikon), and confocal images were acquired using an inverted SP5X confocal microscope and a 63× objective lens (HCX PL APO CS, oil immersion, 1.4 NA; Leica) with the optical section thickness set at 1 μm. Microscopy imaging was initiated typically 3 min after mixing GUVs and wheat germ lysates.

To quantify the phase preferences of PH-GFP and Gag-YFP, we determined the fractions of fluorescent proteins partitioning to the DiD(+) phase [%DiD(+)]. Briefly, the fluorescence intensities of fluorescent protein bound to DiD(+) and DiD(−) phases were measured based on intensity line profiles along a randomly drawn line crossing DiD(+) and DiD(−) phases of the GUVs in confocal images. From these values, the background values (an average intensity for the 3-μm region outside the GUV along the line) were subtracted to yield $F_{DiD(+)}$ and$F_{DiD(-)}$. These values were used to calculate %DiD(+) by using the following equation: $\%DiD(+) = F_{DiD(+)}/[F_{DiD(+)} + F_{DiD(-)}] \times 100$. A similar analysis was previously performed to quantify protein partitioning to GUV phases (29, 30).

Incorporation of myristate. To test whether wheat germ lysates support myristoylation of Gag proteins, either WT Gag-YFP or 1GA Gag-YFP, which lacks the myristoylation site, was translated in the presence of [^{35}S]methionine-cysteine or [^{3}H]myristic acid (myristic acid, [9,10-^{3}H(N)]; PerkinElmer). After the reaction, the lysates containing translated proteins were separated by SDS-PAGE and subjected to autoradiography for detection of synthesized Gag-YFP proteins and incorporated myristic acid.

Liposome-binding assay. The liposome-binding assay was performed as previously described (3), except that in the present study, 12.5-μl aliquots of wheat germ lysates containing WT Gag-YFP diluted to 25 μl with 20 mM HEPES were used in place of 25 μl of rabbit reticulocyte lysate-based *in vitro* transcription and translation reaction mixtures. Preparation of liposomes and sucrose gradient flotation centrifugation were performed as described previously (3). Following centrifugation, a total of five fractions were collected from the top of the gradient, and the proteins were separated by SDS-PAGE followed by phosphorimaging analysis.

RESULTS

Efficient binding of HIV-1 Gag-YFP to GUVs requires treatment of Gag-YFP with RNase or the presence of PI(4,5)P_2. We previously demonstrated that binding of HIV-1 Gag to liposomes containing a 2:1 ratio of POPC and POPS requires the presence of PI(4,5)P_2 lipids (3, 18, 20). If Gag is treated with RNase, however, POPS mediates the efficient binding of Gag to liposomes lacking PI(4,5)P_2 (18). Notably, the liposome membranes used in these assays have an opposite curvature than the inner leaflet of the PM, on which viral assembly occurs in cells. As the liposomes used in the previous studies had small diameters (<200 nm), the steep opposite curvature may have imposed a stringent requirement for Gag binding, which might not be present under native conditions. Importantly, membrane curvature affects phosphoinositide-dependent membrane binding of several proteins (31–33). To determine whether steep curvature necessitates PI(4,5)P_2 or RNA removal, we examined Gag-membrane interactions using GUVs whose membranes are essentially flat on the size scale of a Gag protein. We synthesized full-length Gag tagged with the Venus variant of YFP (here referred to as Gag-YFP) via *in vitro* translation reactions using wheat germ lysates. We confirmed that the wheat germ lysates supported N-terminal myristoylation of Gag-YFP (Fig. 1A), as reported previously (34), and that in liposome flotation assays, Gag-YFP synthesized in wheat germ lysates bound to liposomes in a PI(4,5)P_2-dependent manner (Fig. 1B). To examine the requirement for Gag-YFP binding to GUVs consisting of POPC and POPS, we mixed Gag-YFP-containing wheat germ lysates with GUVs and imaged the mixtures under a confocal microscope. We found that WT Gag-YFP failed to bind to GUVs consisting of POPC, POPS, and cholesterol (POPC+POPS+chol) (Fig. 1C). In contrast, WT Gag-YFP treated with RNase bound efficiently to the POPC+POPS+chol GUVs (Fig. 1D), in good agreement with observations from liposome flotation assays. Addition of RNase alone did not cause apparent changes in the POPC+POPS+chol GUVs, which were visualized by inclusion of a fluorescent lipid probe for DiD (data not shown). These results suggested that RNA inhibits binding of WT Gag-YFP to PS-containing membranes regardless of membrane curvature.

To test whether the requirement for PI(4,5)P_2 also applies to Gag-YFP binding to GUVs, we prepared POPC+POPS+chol GUVs that also contain PI(4,5)P_2 purified from porcine brain [referred to as brain-PI(4,5)P_2]. We found that without RNase treatment, binding of WT Gag-YFP to GUVs containing 10 mol% brain-PI(4,5)P_2 (Fig. 1E) but not to GUVs lacking PI(4,5)P_2 (Fig. 1C) was readily detectable 3 min after mixing. This binding required myristoylation of Gag-YFP, as a nonmyristoylated Gag-YFP mutant showed no GUV binding (data not shown). While GUVs containing 2.5% or 5% brain-PI(4,5)P_2 also supported Gag-YFP binding, this required longer incubation periods (~30 min), at the end of which many GUVs ruptured. The instability of similar GUVs has been noted in the other studies as well (35). Therefore, GUVs containing 10% PI(4,5)P_2 were used in most of the subsequent experiments. Of note, 10% PI(4,5)P_2 was recently used to establish a robust GUV-based assay system that allows comparison of clathrin coat formation in the presence of different PI(4,5)P_2-binding adapter proteins (36).

The requirement for PI(4,5)P_2 has also been observed in other studies examining GUV binding of Gag or MA (35, 37), which confirms previous liposome flotation studies showing that matching the overall charge of GUVs by increasing the PS content does not circumvent the PI(4,5)P_2 requirement (3). Interestingly, one of these studies showed that MA binding to GUVs requires addition of a heterologous dimerization motif to the MA domain (35). The CA domain in Gag forms a dimerization interface, whereas the NC domain promotes higher-order Gag multimerization (38, 39). To test the role of the latter, we examined a Gag-YFP derivative lacking the majority of NC (delNC), which was capable of substantial membrane binding but showed diminished Gag multimerization in cells, as evidenced by reduced Gag-CFP-Gag-YFP fluorescence resonance energy transfer and defects in virus-like particle release (28). We observed that delNC Gag-YFP bound to GUVs in an RNase- and PI(4,5)P_2-dependent manner, like WT Gag-YFP (Fig. 1F to H), suggesting that the observed PI(4,5)P_2- or RNase-dependent binding of WT Gag to GUVs is not dependent on higher-order Gag multimerization. Together, these results suggested that Gag binding to the POPC+POPS+chol membranes is dependent on either RNA removal from Gag or the presence of PI(4,5)P_2, regardless of membrane curvature, and that this binding does not require the NC domain.

Acyl chains of PI(4,5)P_2 play a major role in PI(4,5)P_2-medi-

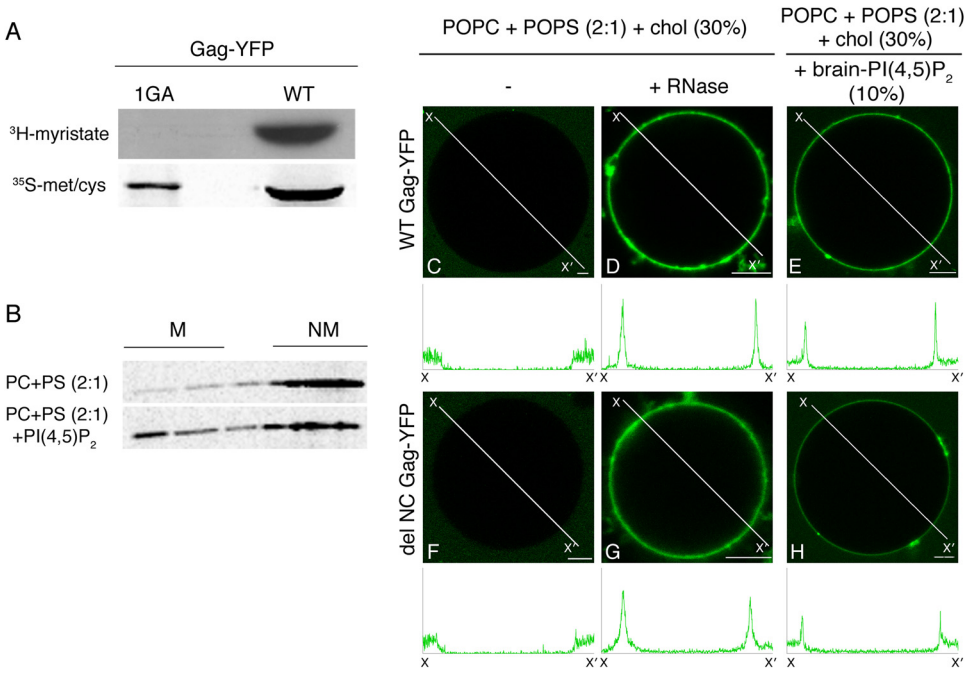

FIG 1 Either RNA removal or the presence of $PI(4,5)P_2$ in membranes promotes binding of Gag to POPS-based GUVs. (A) Myristoylation of WT and 1GA Gag-YFP synthesized *in vitro* using wheat germ lysate was examined as described in Materials and Methods. (B) Liposome-binding assays were performed to confirm that WT Gag-YFP synthesized in wheat germ lysates binds liposomes in a $PI(4,5)P_2$-dependent manner, as has been observed for Gag synthesized in rabbit reticulocyte lysates. Wheat germ lysates containing WT Gag-YFP were mixed with liposomes of the indicated compositions, and membrane-bound (M) and non-membrane-bound (NM) proteins were fractionated by sucrose gradient flotation centrifugation performed as described in Materials and Methods. Following centrifugation, a total of five fractions were collected from the top of the gradient, and the proteins were separated by SDS-PAGE followed by phosphorimager analysis. (C to H) Wheat germ lysates containing either WT Gag-YFP (C to E) or delNC Gag-YFP (F to H) were mixed with GUVs composed of the indicated sets of lipids. Lipid ratios used were as follows: POPC:POPS:chol, 46.6:23.3:30 (C, D, F, and G); POPC:POPS:chol:$PI(4,5)P_2$, 40:20:30:10 (E and H). Images were acquired using a confocal microscope. Binding of WT Gag-YFP (C and D) or delNC Gag-YFP (F and G) to POPC+POPS+chol GUVs was examined without (C and F) or with addition of RNase (final concentration, 10 μg/μl) (D and G). Binding of either WT Gag-YFP (E) or delNC Gag-YFP (H) to POPC+POPS+chol+brain-$PI(4,5)P_2$ GUVs was examined as described above. Representative images from at least 3 independent experiments are shown. Fluorescence intensity profiles along the lines drawn to cross over opposite sides of GUVs (X to X′) are shown below the images. Bar, 5 μm.

ated membrane binding of Gag-YFP but not in membrane binding of PH-GFP. To examine whether acyl chain types of $PI(4,5)P_2$ affect Gag-membrane interactions, we compared Gag-YFP binding to GUVs containing three different acyl chain variants of $PI(4,5)P_2$: brain-$PI(4,5)P_2$, which is predominantly composed of saturated (stearoyl) and unsaturated (arachidonyl) acyl chains; dioleoyl-$PI(4,5)P_2$ [DO-$PI(4,5)P_2$] with two unsaturated oleoyl acyl chains; dipalmitoyl-$PI(4,5)P_2$ [DP-$PI(4,5)P_2$] with two saturated (palmitoyl) acyl chains. $PI(4,5)P_2$ incorporation into GUVs was tested using PH-GFP, a GFP fusion with the $PH_{PLC\delta_1}$ domain. This construct has been used as a specific probe for $PI(4,5)P_2$ in many experimental systems, including those using GUVs (40, 41). PH-GFP binding confirmed the incorporation of $PI(4,5)P_2$ with different acyl chains into GUVs (Fig. 2B to D). As expected, GUVs lacking $PI(4,5)P_2$ did not support binding of either PH-GFP or WT Gag-YFP (Fig. 2A and E). In contrast, binding of WT Gag-YFP to GUVs containing either brain-$PI(4,5)P_2$ (Fig. 2F) or DO-$PI(4,5)P_2$ (Fig. 2G) was readily detected. Remarkably, however, we found that WT Gag-YFP did not bind GUVs containing DP-$PI(4,5)P_2$ (Fig. 2H). These results indicate that acyl chains of $PI(4,5)P_2$ play an important role in $PI(4,5)P_2$-mediated membrane binding of Gag. The observed acyl chain preference does not appear to require higher-order Gag multimerization, since delNC Gag-YFP showed the same preference (Fig. 2I to L).

RNase-treated Gag-YFP shows nonuniform binding to DPPS-containing GUVs. To test whether PS with fully saturated acyl chains also fail to support Gag binding to GUVs, we examined POPC+DPPS+chol GUVs for binding of Gag-YFP upon RNase treatment. High-melting-temperature lipids such as DPPS (T_m = 54°C) tend to form a tightly packed phase known as the gel phase (42–45), which can be visually separated from a coexisting liquid phase based on exclusion of a fluid-phase lipid dye. Indeed, when the fluid-phase probe DiD was included in POPC+DPPS+chol GUVs, DiD(+) (liquid) and DiD(−) phases were readily distinguished (Fig. 3A), in contrast to the POPC+POPS+chol GUVs used above, which showed a uniform DiD distribution (data not shown). FITC-polylysine, a fluorophore-conjugated basic polypeptide that binds acidic lipids via electrostatic interactions, bound largely to the DiD(−) phase, suggesting that DPPS is enriched in that phase (Fig. 3B and C). Of note, FITC-polylysine binding revealed that the DiD(−) phase contains some flattened regions separated by higher curvature facets (Fig. 3C), consistent with there being a large bending rigidity. This, in combination with the observation that DiD(−) regions have irregular boundaries (Fig. 3H), suggest that these regions consist of lipids in a tightly packed gel phase (46–49).

In POPC+DPPS+chol GUVs, RNase-treated Gag-YFP showed prominent binding to the DiD(−) but not DiD(+) part of the GUV surface (Fig. 3D and E). RNase-treated delNC Gag-YFP bound to the DiD(−) phase, similar to WT Gag-YFP, suggesting

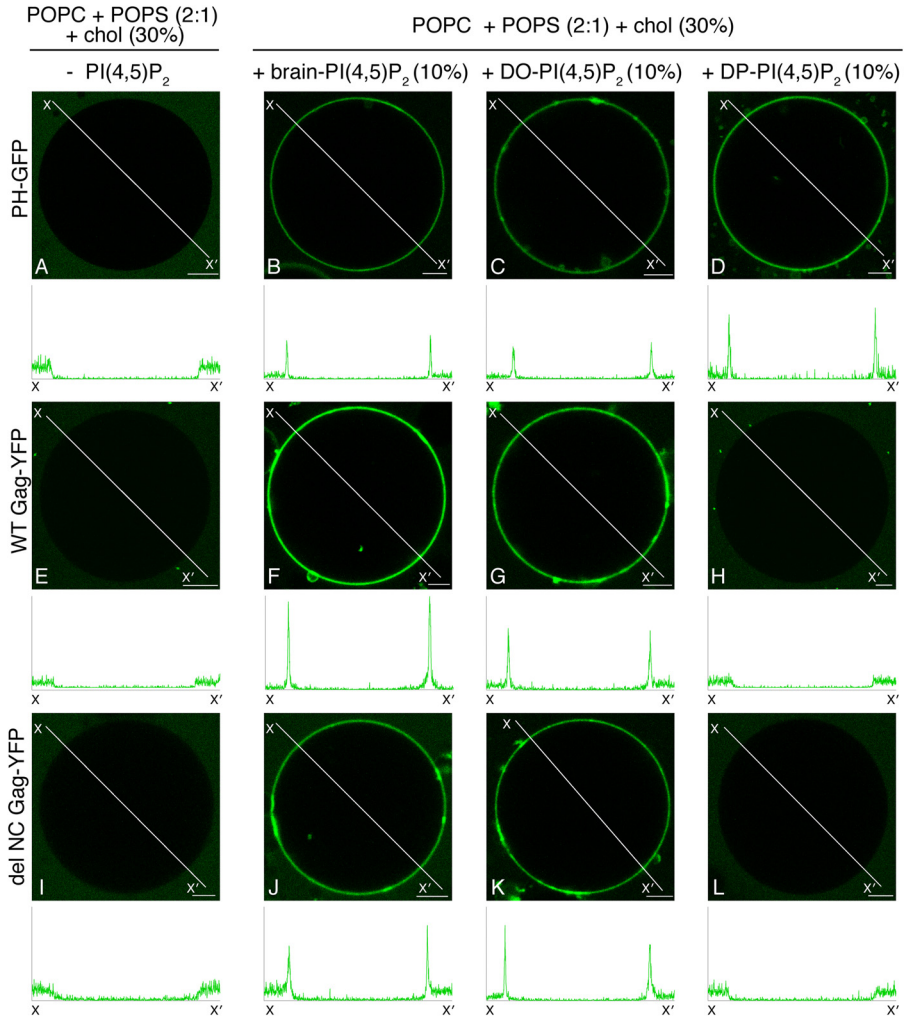

FIG 2 Brain-PI(4,5)P_2 and DO-PI(4,5)P_2, but not DP-PI(4,5)P_2, promote stable binding of Gag to POPS-based GUVs. Binding of either PH-GFP (A to D), WT Gag-YFP (E to H), or delNC Gag-YFP (I to L) to GUVs containing no PI(4,5)P_2 (A, E, and I), brain-PI(4,5)P_2 (B, F, and J), DO-PI(4,5)P_2 (C, G, and K), or DP-PI(4,5)P_2 (D, H, and L) was examined in the context of POPC+POPS+chol GUVs, as in Fig. 1. Lipid ratios used were as follows: POPC:POPS:chol, 46.6:23.3:30 (A, E, and I); POPC:POPS:chol:PI(4,5)P_2, 40:20:30:10 (B to D, F, G, and J to L). Representative images from at least 3 independent experiments are shown. Fluorescence intensity profiles along the lines drawn to cross over opposite sides of GUVs (X to X′) are shown below images. PH-GFP and WT and delNC Gag-YFP were imaged using the same confocal microscopy settings, and their line profiles are shown on the same *y* axis scale. Bar, 5 μm.

that higher-order multmerization is not necessary for binding to the DiD(−) phase (Fig. 3F and G). Altogether, these results indicate that POPC+DPPS+chol GUVs form DiD(+) liquid and DiD(−) gel phases, the latter of which is enriched in DPPS and recruits Gag efficiently when RNA is removed from Gag.

Gag-YFP but not PH-GFP is distributed uniformly on DPPS-containing two-phase GUVs in the presence of brain-PI(4,5)P_2. We next examined the role of PI(4,5)P_2 in POPC+DPPS+chol two-phase GUVs. GUVs containing brain-PI(4,5)P_2 showed coexisting DiD(+) and DiD(−) phases at room temperature (Fig. 4E and G), as was observed for GUVs lacking PI(4,5)P_2 (Fig. 3). PH-GFP bound to the DiD(+) phase in these GUVs (Fig. 4F), suggesting that PI(4,5)P_2 is present in the DiD(+) phase. As expected, Gag-YFP showed readily detectable binding to the DiD(+) phase (Fig. 4H), which also supported binding of PH-GFP. Remarkably, we also observed additional binding of Gag-YFP to the DiD(−) phase in these GUVs, despite the observation that PH-GFP does not bind to this phase (Fig. 4E, F, G, and H). A quantitative analysis based on confocal microscopy images (Fig. 4I) indicated that while PH-GFP strongly prefers the DiD(+) phase, Gag-YFP distributes to both the DiD(+) and DiD(−) phases at similar levels (Fig. 4J).

Gag-YFP did not bind the DiD(−) phase of POPC+DPPS+chol GUVs in the absence of PI(4,5)P_2 (Fig. 4C and D) unless treated with RNase (Fig. 3D and E), suggesting a role for PI(4,5)P_2 in Gag-YFP binding to the DiD(−) phase (Fig. 4H). To test whether an interaction with PI(4,5)P_2 is necessary for efficient Gag binding to the DPPS-enriched DiD(−) phase of two-phase GUVs, we examined GUV binding of HBR/RKswitch Gag-YFP, in which lysines and arginines in MA HBR are switched. Our previous study using liposome flotation assays showed that this Gag derivative fails to bind to PI(4,5)P_2 but retains the ability to bind PS upon RNase treatment (6). Therefore, if an interaction with PI(4,5)P_2 were necessary for binding of Gag to the DPPS-enriched DiD(−) phase, HBR/RKswitch Gag-YFP would be expected to fail to bind the DiD(−) phase. Indeed, using brain-PI(4,5)P_2-con-

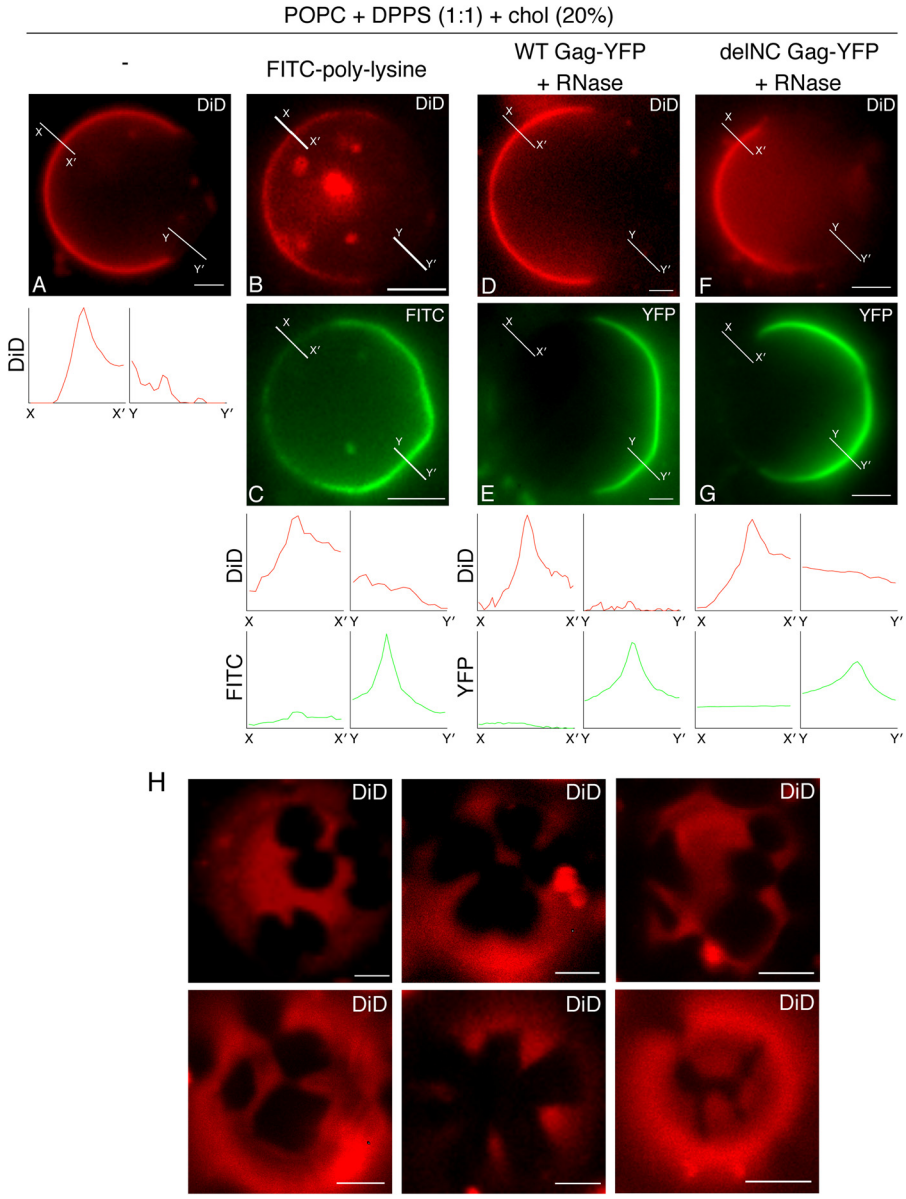

FIG 3 In the absence of PI(4,5)P_2, Gag binds to the DPPS-enriched DiD(−) phase after RNase treatment. (A) An example of an epifluorescence image of POPC+DPPS+chol+DiD GUVs containing DiD(+) and DiD(−) phases. (C) Binding of FITC-polylysine to POPC+DPPS+chol GUVs. (E and G) Binding of either WT Gag-YFP (E) or delNC Gag-YFP (G) to POPC+DPPS+chol GUVs was examined after RNase treatment. (B, D, and F) Corresponding images of DiD. The lipid ratio used was as follows: POPC:DPPS:chol, 40:40:20. Representative images from at least 3 independent experiments are shown. Fluorescence intensity profiles of DiD (red) and FITC or YFP (green) along the short lines drawn to cross over DiD(+) (X to X′) and DiD(−) (Y to Y′) regions of GUVs are shown below the images. (H) Six examples of confocal images of the top surface of POPC+DPPS+chol GUVs (POPC:DPPS:chol, 40:40:20) containing DiD are shown. Note that these two-phase GUVs displayed irregularly shaped DiD(−) phases. Bar, 5 μm.

taining two-phase GUVs, we found that HBR/RKswitch Gag-YFP failed to bind not only to the DiD(+) phase but also to the DiD(−) phase (Fig. 4K and L). In contrast, when treated with RNase, HBR/RKswitch Gag-YFP bound both phases (Fig. 4M and N), confirming that this Gag-YFP derivative is capable of binding to acidic lipids present in both phases after RNA removal. These results collectively indicate that not only the presence of PI(4,5)P_2 in the GUVs but also the ability of Gag to bind PI(4,5)P_2 are necessary for WT Gag binding to the DPPS-enriched phase, even though this phase does not support binding of PH-GFP.

PI(4,5)P_2 directs PH-GFP and Gag-YFP to different phases in two-phase GUVs in an acyl chain-dependent manner. To examine whether the preference of Gag for PI(4,5)P_2 with unsaturated acyl chains observed with single-phase GUVs would also occur with two-phase GUVs, we replaced brain-PI(4,5)P_2 with either DO-PI(4,5)P_2 or DP-PI(4,5)P_2 in the two-phase GUVs examined above. PH-GFP bound preferentially to the DiD(+) phase in these two-phase GUVs (Fig. 4J and 5A, B, E, and F), indicating the presence of PI(4,5)P_2 in the DiD(+) phase; however, we noted the possibility that binding of PH-GFP to PI(4,5)P_2 is somehow suppressed in the context of the DiD(−) gel phase. Consistent with the results obtained with the single-phase GUVs, DO-PI(4,5)P_2

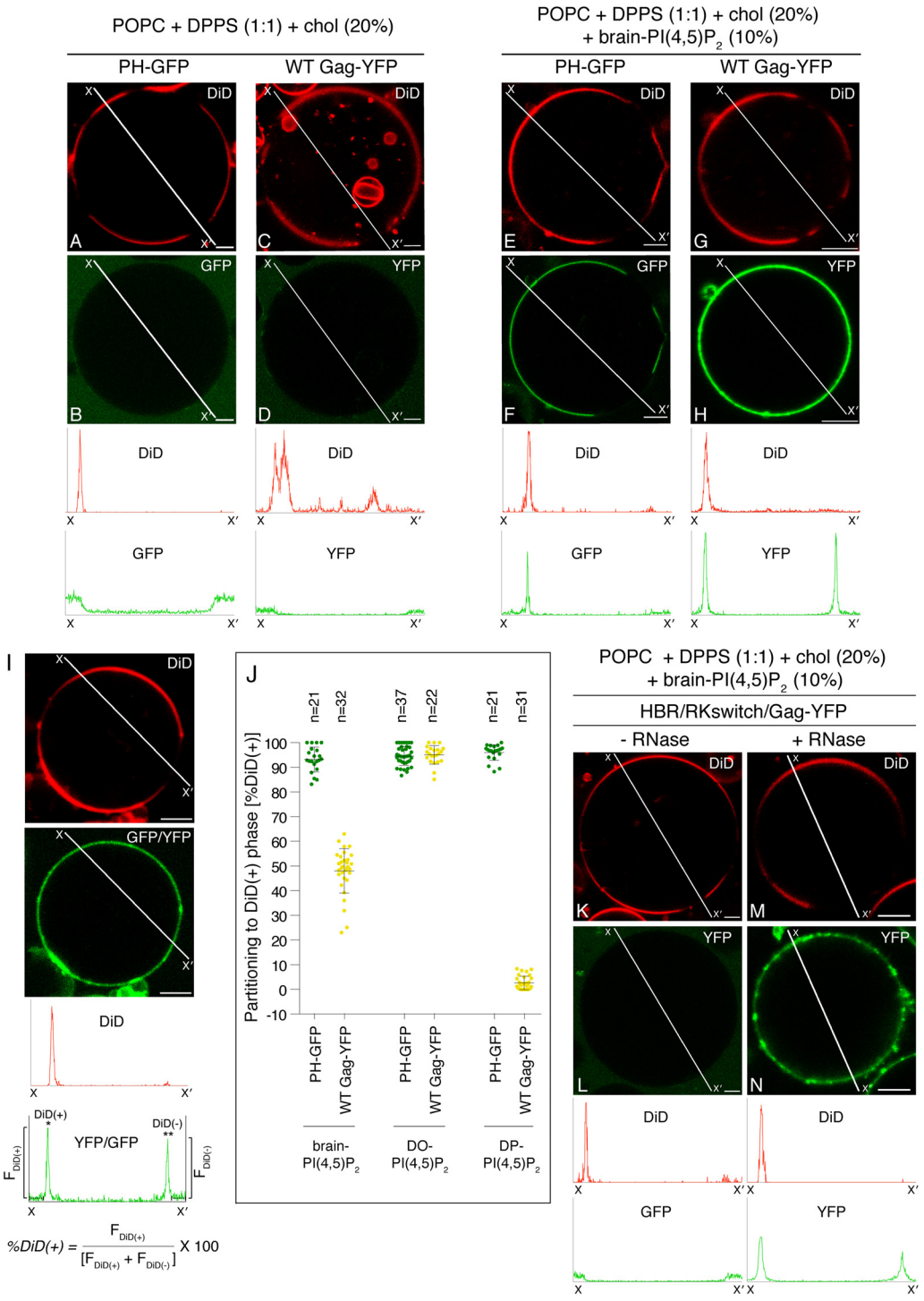

FIG 4 Gag-YFP and PH-GFP distribute differently in DPPS-containing two-phase GUVs in the presence of brain-PI(4,5)P_2. (A to H) POPC+DPPS+chol (A to D) and POPC+DPPS+chol+brain-PI(4,5)P_2 (E to H) GUVs were examined for binding of PH-GFP (B and F) and WT Gag-YFP (D and H) by using confocal microscopy. PH-GFP and WT Gag-YFP were imaged using the same microscopy settings. Corresponding images of DiD are shown in panels A, C, E, and G. Representative images from at least 3 independent experiments are shown. Fluorescence intensity profiles of PH-GFP and Gag-YFP along the lines drawn to cross over DiD(+) and DiD(−) sides of GUVs (X to X′) are shown below the images in the same *y* axis scale. (I) The method for calculating partitioning of GFP or YFP signals to the DiD(+) phase is illustrated. Examples of confocal images of DiD and GFP or YFP (Gag-YFP in this example) associated with a two-phase GUV [containing brain-PI(4,5)P_2 in this example] are shown in the top two panels. The intensity profiles of DiD (red) and GFP/YFP (green) along the line crossing DiD(+) and DiD(−) phases (X to X′) are shown below the images. Average intensity values along the 3-μm segments of the line outside the DiD(+) and DiD(−) phases (indicated by short broken lines on the intensity profile plot) were subtracted from DiD(+) (*) and DiD(−) (**) peak intensity values to obtain $F_{DiD(+)}$ and $F_{DiD(-)}$, respectively. These values were used to calculate partitioning to the DiD(+) phase [%DiD(+)] using the relation shown below the profile plot. (J) Partitioning of PH-GFP (green) or WT Gag-YFP (yellow) to the DiD(+) phase in POPC+DPPS+chol GUVs containing brain-, DO-, or DP-PI(4,5)P_2 were quantified for each GUV as described in Materials and Methods and for panel I. Means ± standard deviations are also shown. *n*, the number of GUVs analyzed under each condition. (K to N) Binding of the HBR/RKswitch Gag-YFP to POPC+DPPS+chol+brain-PI(4,5)P_2 GUVs was examined without (L) or with (N) RNase treatment. Corresponding images of DiD are shown in panels K and M. Representative images from at least 3 independent experiments are shown. Fluorescent intensity profiles of DiD (red) and Gag-YFP (green) along the lines drawn as described above are shown below the images. Bar, 5 μm. Lipid ratios used were as follows: POPC:DPPS:chol, 40:40:20 (A to D); POPC:DPPS:chol:PI(4,5)P_2, 35:35:20:10 (E to H and K to N).

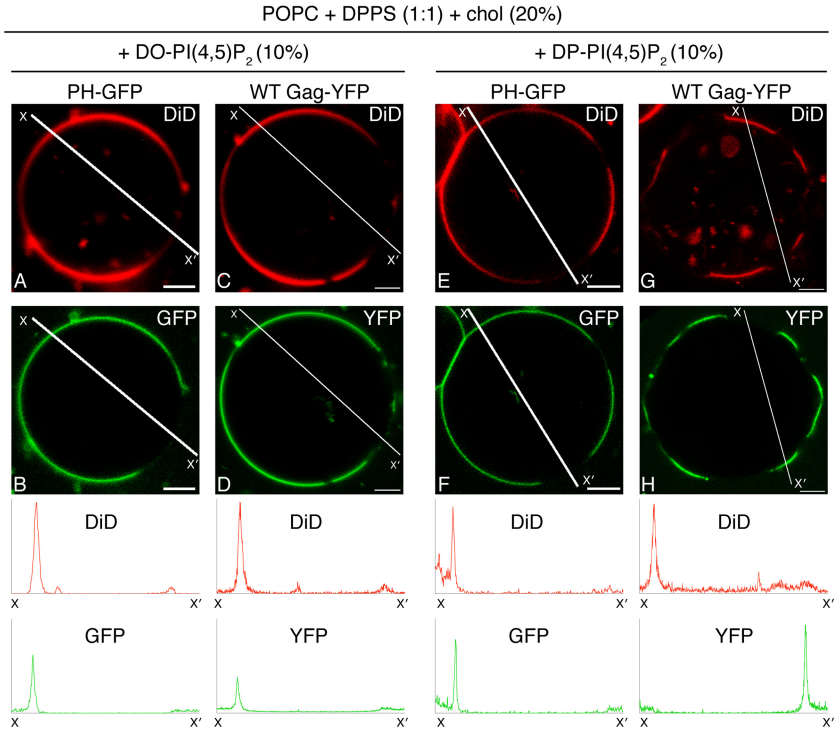

FIG 5 DP-PI(4,5)P_2, but not DO-PI(4,5)P_2, directs PH-GFP and WT Gag-YFP to different phases in two-phase GUVs. Binding of PH-GFP (B and F) and WT Gag-YFP (D and H) to POPC+DPPS+chol+DO-PI(4,5)P_2 (A to D) and POPC+DPPS+chol-DP+DP-PI(4,5)P_2 (E to H) GUVs was examined using confocal microscopy. PH-GFP and WT Gag-YFP were imaged using the same microscopy settings. (A, C, E, and G) Corresponding images of DiD. Representative images from at least 3 independent experiments are shown. Fluorescence intensity profiles of DiD (red) and PH-GFP or Gag-YFP (green) along the lines drawn to cross over DiD(+) and DiD(−) sides of GUVs (X to X′) are shown below the images. The intensity profiles for PH-GFP and Gag-YFP are shown on the same *y* axis scale. Partitioning of PH-GFP and WT Gag-YFP to the DiD(+) phase in POPC+DPPS+chol GUVs containing either DO or DP PI(4,5)P_2 was quantified, and the results were included in Fig. 4J. Bar, 5 μm. The lipid ratio used was as follows: POPC:DPPS:chol:PI(4,5)P_2, 35:35:20:10.

supported stable binding of Gag-YFP (Fig. 5D). In these GUVs, Gag-YFP bound to the DiD(+) phase (Fig. 5C and D), as observed for PH-GFP (Fig. 5A and B), suggesting that DO-PI(4,5)P_2 present in this phase recruits both proteins. Surprisingly, in contrast to the results obtained with single-phase GUVs, binding of Gag-YFP to two-phase GUVs containing DP-PI(4,5)P_2 was readily detected (Fig. 5H). Moreover, in clear contrast to PH-GFP (Fig. 5E and F), we found that Gag-YFP localized to the DiD(−) phase (Fig. 4J and 5G and H). A similar Gag distribution was also observed when total DP-PI(4,5)P_2 was reduced to 5% (data not shown). Altogether, these results further highlight the differences between Gag and PH-GFP in their responses to acyl chain variants of PI(4,5)P_2.

The N-terminal myristate moiety does not play a major role in determining the dependence of Gag membrane binding on unsaturated PI(4,5)P_2 acyl chains. The observed differences between PI(4,5)P_2 with an unsaturated acyl chain and DP-PI(4,5)P_2 in supporting Gag-membrane binding may be mediated either by a direct mechanism dependent on MA-PI(4,5)P_2 interactions or by an indirect mechanism involving the N-terminal myristate moiety. We previously showed that nonmyristoylated 1GA Gag is capable of binding to PS-containing liposomes after RNase treatment (18). To examine whether the dependence of Gag-GUV binding on PI(4,5)P_2 acyl chain unsaturation involves the N-terminal myristate moiety, we tested binding of RNase-treated 1GA Gag-YFP to POPC+chol+PI(4,5)P_2 GUVs containing either brain-PI(4,5)P_2 or DP-PI(4,5)P_2 as the sole acidic lipid. As expected, 1GA Gag-YFP bound to neither brain-PI(4,5)P_2-containing (Fig. 6D) nor DP-PI(4,5)P_2-containing (Fig. 6J) GUVs without RNase treatment. However, as observed previously in liposome-binding assays (18), RNase-treated 1GA Gag-YFP bound to brain-PI(4,5)P_2-containing GUVs (Fig. 6F). In contrast, RNase-treated 1GA Gag-YFP failed to bind DP-PI(4,5)P_2-containing GUVs (Fig. 6L). PH-GFP bound to both brain PI(4,5)P_2-containing (Fig. 6B) and DP-PI(4,5)P_2-containing (Fig. 6H) GUVs, indicating that both PI(4,5)P_2 variants are accessible to PH-GFP. These results suggest that indirect mechanisms requiring myristate are unlikely to determine the dependence of Gag membrane binding on (un)saturation of PI(4,5)P_2 acyl chains.

DISCUSSION

In this study, we examined binding of two PI(4,5)P_2-binding proteins, HIV-1 Gag and PH-GFP, to membranes containing acyl chain variants of PI(4,5)P_2 in single- and two-phase GUVs. Consistent with two recent GUV-based studies (35, 37), we found that PI(4,5)P_2 is essential for Gag binding to membranes regardless of membrane curvature. Furthermore, we found that in addition to the headgroup, the acyl chains of PI(4,5)P_2 also play an important role in Gag binding to membranes. We observed that brain-PI(4,5)P_2 and DO-PI(4,5)P_2 but not DP-PI(4,5)P_2 support Gag binding to single-phase GUV membranes (Fig. 7). Interestingly, our study also revealed that variations in acyl chains of PI(4,5)P_2

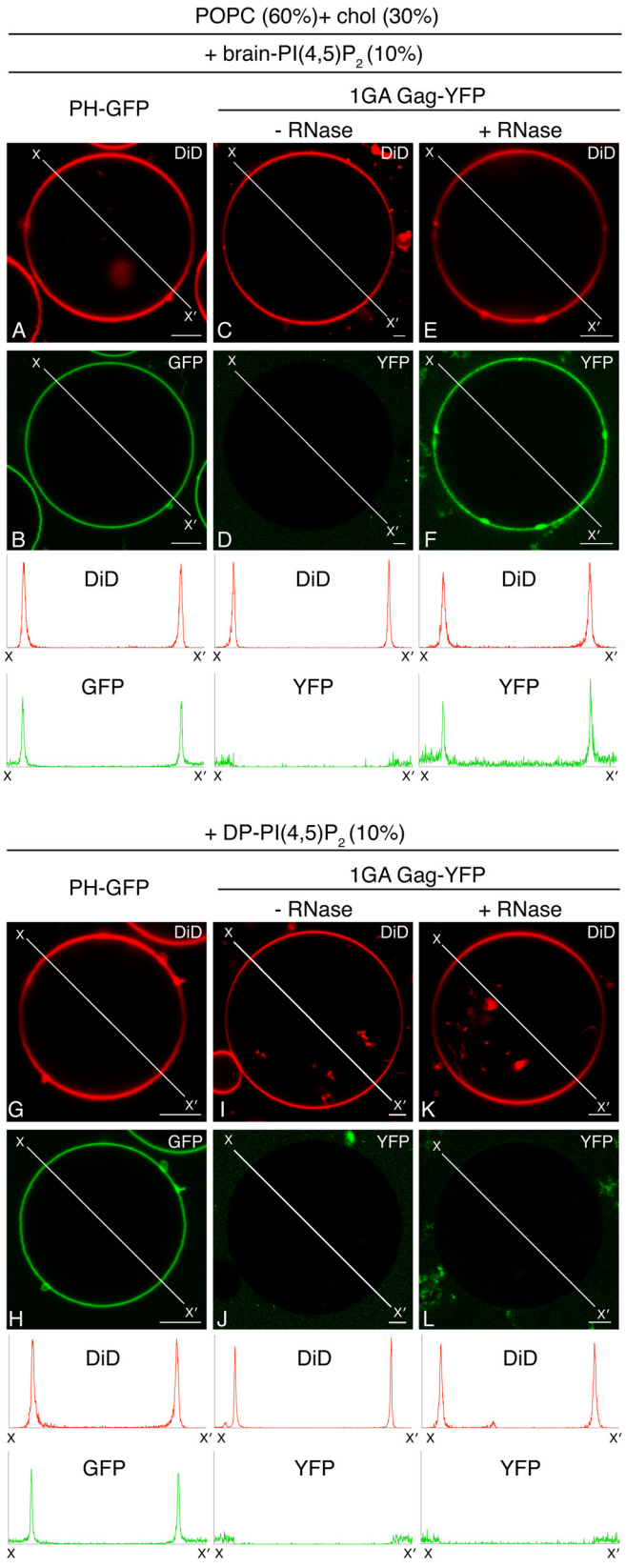

FIG 6 RNase-treated 1GA Gag-YFP binds to GUVs containing brain-PI(4,5)P_2 but not DP-PI(4,5)P_2 as a sole acidic lipid. Binding of PH-GFP (B and H), 1GA Gag-YFP (D and J), and RNase-treated 1GA Gag-YFP (F and L) to either POPC+chol+brain-PI(4,5)P_2 (B, D, and F) or POPC+chol+DP-PI(4,5)P_2 (H, J, and L) GUVs were examined using confocal microscopy. PH-GFP and 1GA Gag-YFP were imaged using the same microscopy settings. Corresponding images of DiD are shown in panels A, C, E, G, I, and K. Representative images from at least 3 independent experiments are shown. Fluorescence intensity profiles of DiD (red) and PH-GFP or Gag-YFP (green) along the lines drawn to cross over opposite sides of GUVs (X to X′) are shown below. The intensity profiles for PH-GFP and Gag-YFP are shown on the same *y* axis scale. The lipid ratio used was as follows: POPC:chol:PI(4,5)P_2, 60:30:10. Bar, 5 μm.

affect the localization of Gag, but not PH-GFP, to different phases distinguished by DiD in two-phase GUVs. To our knowledge, this is the first study to demonstrate biochemically that membrane-binding behaviors of proteins that bind PI(4,5)P_2 are differentially modulated by acyl chains of this acidic phospholipid, which is involved in a wide variety of cellular functions.

The inability of DP-PI(4,5)P_2 to support stable binding of Gag to single-phase GUVs suggests that unsaturated acyl chains of PI(4,5)P_2 are necessary for PI(4,5)P_2-dependent Gag retention at the membrane. What is the potential mechanism by which saturation of PI(4,5)P_2 acyl chains prevents stable Gag membrane binding? The N-terminal myristate moiety, which mediates hydrophobic interactions with the lipid bilayer, plays an important role in membrane binding of Gag. A previous study suggested that unlike the saturated myristate moiety, unsaturated analogs do not support proper Gag localization, presumably because of mismatching with the lipid bilayer environment (50). It is conceivable that DP-PI(4,5)P_2 may create a bilayer environment that disfavors insertion of even the saturated myristoyl moiety in the immediate surrounding area and thereby reduce stability of Gag membrane binding. However, we observed that the RNase-treated, nonmyristoylated Gag derivative, which can bind PS-containing membrane (18), bound GUVs containing brain-PI(4,5)P_2 but not those containing DP-PI(4,5)P_2 when PI(4,5)P_2 was the sole acidic lipid in GUVs (Fig. 6). These results suggest that MA-PI(4,5)P_2 interactions determine Gag preference for PI(4,5)P_2 with unsaturated acyl chains and that the myristate moiety plays only a minor role, if any. Earlier solution NMR studies of MA complexed with short acyl chain derivatives of PI(4,5)P_2 suggested that the MA globular domain can sequester the sn-2 acyl chain of PI(4,5)P_2, a majority of which is unsaturated in cells (4). This acyl chain sequestration may contribute to stable interactions of Gag with PI(4,5)P_2 (4, 13). In such case, it is conceivable that Gag is able to sequester only unsaturated but not saturated acyl chains. For example, a saturated acyl chain may encounter a steric hindrance within the MA globular domain or a higher energetic barrier against extrusion from lipid bilayers. In case the acyl chain sequestration by MA is not involved (as shown *in silico* by Charlier et al. recently [51]), saturated acyl chains may affect Gag membrane binding by altering the orientation of or distance between PI(4,5)P_2 molecules or their headgroups. At pH 7.3, which is the pH of the wheat germ lysate-GUV mixtures, PI(4,5)P_2 self-clusters, according to several *in vitro* studies (52–54). Therefore, it is possible that the observed effect of acyl chain saturation on Gag binding to PI(4,5)P_2 may involve clustering (or lack thereof) of this lipid.

In contrast to the findings of the current study, Alfadhli et al. observed that myristoylated MACA purified from bacterial lysates binds to DP-PI(4,5)P_2-containing membranes nearly as efficiently as membranes containing DO or brain PI(4,5)P_2 in sonicated liposome-based assays (24). Of note, although myristoylated MACA lacks the NC domain, which can modulate Gag membrane

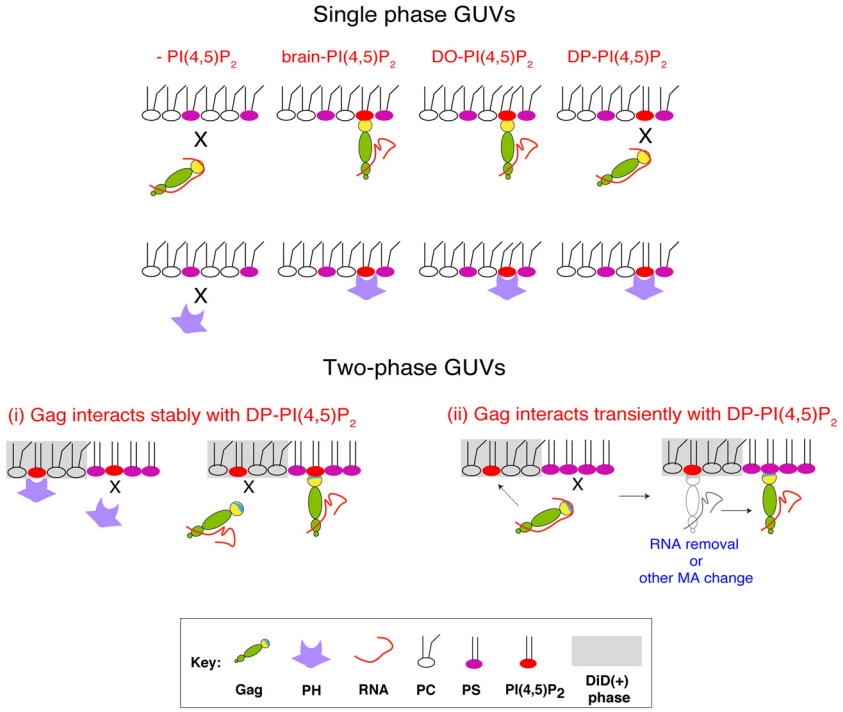

FIG 7 Acyl chains of $PI(4,5)P_2$ differentially affect membrane binding of Gag and PH-GFP. Schematic representation of Gag and PH-GFP binding to single-phase GUVs (top) and two-phase GUVs (bottom) with different acyl chain variants of $PI(4,5)P_2$ are illustrated. In the bottom panel, two mutually nonexclusive potential mechanisms by which DP-$PI(4,5)P_2$ mediates membrane binding of Gag in two-phase GUVs are depicted. For mechanism i, DP-$PI(4,5)P_2$ in the DiD(−) phase supports stable membrane binding of Gag but not PH-GFP. Conversely, DP-$PI(4,5)P_2$ in the DiD(+) phase supports stable membrane binding of PH-GFP but not Gag. For mechanism ii, DP-$PI(4,5)P_2$ interacts with Gag only transiently, which enables Gag to bind DPPS in the DiD(−) phase. While not depicted, the same process can take place when DP-$PI(4,5)P_2$ is also in the DiD(−) phase. Again, DP-$PI(4,5)P_2$ in the DiD(+) phase, but not in the DiD(−) phase, supports stable binding of PH-GFP (not depicted).

binding, it is unlikely that NC gave rise to the different outcomes, because deletion of NC did not alter the acyl chain preference observed with WT Gag in our experiments using single-phase GUVs (Fig. 2J to L). We speculate that the differences in Gag protein preparation and/or membrane properties between this other study and ours may account for the different outcomes. Identifying the key technical differences may help us understand how Gag distinguishes $PI(4,5)P_2$ acyl chains.

GUVs containing coexisting liquid-ordered (L_o) and liquid-disordered (L_d) phases are often used to examine the characteristics of lipid rafts or molecules that associate with them (35). Lipid rafts are membrane microdomains enriched in cholesterol and saturated lipids and are therefore likely to adopt L_o-like structures due to cholesterol-lipid interactions. However, the two-phase GUVs used in the current study are likely to have coexisting gel and liquid phases rather than L_o and L_d phases. With a gel-to-liquid transition temperature over 50°C (55), one study showed that DPPS is dominant in a gel phase in liposomes consisting of POPC, DPPS, and cholesterol, and does not interact with cholesterol favorably (44). Although the system used in that study is different from ours, we also observed that the DiD(−) phase adopts irregular (not round) shapes that are typical of gel phases (Fig. 3H) (46–49). It is of note that we cannot exclude from these observations the possibility that the DiD(−) phase may contain both L_o and gel phases or have more complex phase behaviors. In either case, while the interaction between MA and the sn-2 acyl chain of $PI(4,5)P_2$ is hypothesized to promote lateral transition of Gag into lipid rafts (4), our system is not suited for testing this intriguing model for Gag-membrane-microdomain interactions, unlike other two-phase GUVs consisting of L_o and L_d phases. Of note, a recent study by Keller et al. (35) observed no transition of Gag derivatives from the L_d to the L_o phase by using GUVs containing $PI(4,5)P_2$. Therefore, diffusion of Gag-$PI(4,5)P_2$ complexes across phase boundaries might not occur even in GUV systems containing two liquid phases.

In two-phase GUVs containing $PI(4,5)P_2$, we found that distributions of Gag and PH-GFP differed depending on the $PI(4,5)P_2$ acyl chain variant used. Both Gag and PH-GFP bound to the DiD(+) phase in DO-$PI(4,5)P_2$-containing two-phase GUVs. This likely reflected the DiD(+) phase localization of DO-$PI(4,5)P_2$, to which both proteins bind. Unlike DO-$PI(4,5)P_2$, however, in DP-$PI(4,5)P_2$-containing two-phase GUVs, Gag strongly preferred the DiD(−) phase, in clear contrast to PH-GFP, which localized to the DiD(+) phase. How does Gag bind to the DPPS-enriched DiD(−) phase, which does not support PH-GFP binding? The results obtained with HBR/RKswitch Gag-YFP (Fig. 4K to N) indicate that Gag localization to this phase still requires a Gag-$PI(4,5)P_2$ interaction. Depending on the nature of this interaction, at least two possibilities can be considered (Fig. 7). In the first possibility (Fig. 7, bottom, i), PH-GFP is unable to detect $PI(4,5)P_2$ molecules present in the DiD(−) phase due either to the scarcity and/or an inhibitory effect of the DPPS milieu. However, the same milieu has a profound enhancing effect on stable DP-$PI(4,5)P_2$-Gag interactions. In another possibility (Fig. 7, bottom,

ii), a transient interaction between Gag and $PI(4,5)P_2$ is sufficient. We and others have shown that Gag can also bind PS after RNA removal (18, 19, 21). *In vitro* studies have supported that $PI(4,5)P_2$ can displace nucleic acids from MA (23, 25). Therefore, it is plausible that even when Gag fails to establish a stable interaction with $PI(4,5)P_2$ [e.g., with DP-$PI(4,5)P_2$], a transient interaction with $PI(4,5)P_2$ molecules present in the DiD(−) phase (which evade the detection by PH-GFP) or those in the DiD(+) phase (detected by PH-GFP) could promote RNA displacement from MA HBR. This in turn enables MA to bind DPPS that is enriched in the DiD(−) phase. These possibilities are not mutually exclusive, and further analyses, including precise determination of lipid contents of both phases, would be required to determine detailed mechanisms.

Acyl chains of PS are also likely to play a role in Gag recruitment to two-phase GUVs containing DP-$PI(4,5)P_2$, since Gag failed to bind to single-phase GUVs that contained DP-$PI(4,5)P_2$. For example, it is conceivable that the DPPS-enriched gel phase affects the orientation of DP-$PI(4,5)P_2$ in the gel phase (in the context of the model shown in Fig. 7, bottom, i) or create the surface with a sufficiently high charge density (Fig. 7, bottom, ii). However, we note that neither DPPS nor DP-$PI(4,5)P_2$ is enriched in virions (56, 57). Therefore, it is unlikely that DP-$PI(4,5)P_2$ would promote Gag membrane binding in cells in a manner observed with the two-phase GUVs. Regardless, however, the results obtained with both single- and two-phase GUV systems support the crucial role played by the saturation status of $PI(4,5)P_2$ acyl chains in Gag membrane binding.

In summary, our data provide evidence that membrane binding of Gag via $PI(4,5)P_2$ is strongly modulated by the acyl chains of $PI(4,5)P_2$ and that the sensitivity to acyl chain saturation differs substantially between the MA domain of HIV-1 Gag and $PH_{PLC\delta_1}$, a representative cellular $PI(4,5)P_2$-binding domain. It is intriguing and important to know whether any other cellular protein show an acyl chain sensitivity similar to that of Gag. Phospholipid acyl chain saturation has been implicated in genome replication and virion infectivity of RNA and DNA viruses (11, 12). Pharmacological inhibition of stearoyl-coenzyme A desaturase (SCD-1), an enzyme that converts saturated to unsaturated acyl chains, was recently shown to suppress HCV replication and hence proposed to be a potential antiviral strategy (58, 59). Likewise, in light of our findings, decreasing the levels of $PI(4,5)P_2$ with unsaturated acyl chains by using a similar strategy may abrogate Gag membrane binding and/or proper Gag localization with minimal effects on cellular $PI(4,5)P_2$-dependent processes. Therefore, further investigations into the differences in mechanisms of $PI(4,5)P_2$ interactions between HIV-1 Gag and cellular $PI(4,5)P_2$-binding domains may open an avenue for therapeutic targeting of Gag-$PI(4,5)P_2$ interactions.

ACKNOWLEDGMENTS

We thank Eric Freed for critical review of the manuscript. We also thank the members of our laboratories for helpful discussions and critical reviews of the manuscript. We thank Mohammed Saleem for advice about electroformation, Krishnan Raghunathan for advice with image analysis, and Ji Yeon J. Chung for technical assistance.

This work is supported by National Institutes of Health grants R01 AI071727 (to A.O.) and R01 GM110052 (to S.L.V).

REFERENCES

1. **Lemmon MA.** 2008. Membrane recognition by phospholipid-binding domains. Nat Rev Mol Cell Biol **9:**99–111. http://dx.doi.org/10.1038/nrm2328.
2. **Ono A, Ablan SD, Lockett SJ, Nagashima K, Freed EO.** 2004. Phosphatidylinositol (4,5) bisphosphate regulates HIV-1 Gag targeting to the plasma membrane. Proc Natl Acad Sci U S A **101:**14889–14894. http://dx.doi.org/10.1073/pnas.0405596101.
3. **Chukkapalli V, Hogue IB, Boyko V, Hu WS, Ono A.** 2008. Interaction between the human immunodeficiency virus type 1 Gag matrix domain and phosphatidylinositol-(4,5)-bisphosphate is essential for efficient gag membrane binding. J Virol **82:**2405–2417. http://dx.doi.org/10.1128/JVI.01614-07.
4. **Saad JS, Miller J, Tai J, Kim A, Ghanam RH, Summers MF.** 2006. Structural basis for targeting HIV-1 Gag proteins to the plasma membrane for virus assembly. Proc Natl Acad Sci U S A **103:**11364–11369. http://dx.doi.org/10.1073/pnas.0602818103.
5. **Shkriabai N, Datta SA, Zhao Z, Hess S, Rein A, Kvaratskhelia M.** 2006. Interactions of HIV-1 Gag with assembly cofactors. Biochemistry **45:**4077–4083. http://dx.doi.org/10.1021/bi052308e.
6. **Llewellyn GN, Grover JR, Olety B, Ono A.** 2013. HIV-1 Gag associates with specific uropod-directed microdomains in a manner dependent on its MA highly basic region. J Virol **87:**6441–6454. http://dx.doi.org/10.1128/JVI.00040-13.
7. **Alfadhli A, Barklis RL, Barklis E.** 2009. HIV-1 matrix organizes as a hexamer of trimers on membranes containing phosphatidylinositol-(4,5)-bisphosphate. Virology **387:**466–472. http://dx.doi.org/10.1016/j.virol.2009.02.048.
8. **Dick RA, Goh SL, Feigenson GW, Vogt VM.** 2012. HIV-1 Gag protein can sense the cholesterol and acyl chain environment in model membranes. Proc Natl Acad Sci U S A **109:**18761–18766. http://dx.doi.org/10.1073/pnas.1209408109.
9. **Ono A, Waheed AA, Freed EO.** 2007. Depletion of cellular cholesterol inhibits membrane binding and higher-order multimerization of human immunodeficiency virus type 1 Gag. Virology **360:**27–35. http://dx.doi.org/10.1016/j.virol.2006.10.011.
10. **Vlach J, Saad JS.** 2013. Trio engagement via plasma membrane phospholipids and the myristoyl moiety governs HIV-1 matrix binding to bilayers. Proc Natl Acad Sci U S A **110:**3525–3530. http://dx.doi.org/10.1073/pnas.1216655110.
11. **Koyuncu E, Purdy JG, Rabinowitz JD, Shenk T.** 2013. Saturated very long chain fatty acids are required for the production of infectious human cytomegalovirus progeny. PLoS Pathog **9:**e1003333. http://dx.doi.org/10.1371/journal.ppat.1003333.
12. **Lee WM, Ahlquist P.** 2003. Membrane synthesis, specific lipid requirements, and localized lipid composition changes associated with a positive-strand RNA virus RNA replication protein. J Virol **77:**12819–12828. http://dx.doi.org/10.1128/JVI.77.23.12819-12828.2003.
13. **Anraku K, Fukuda R, Takamune N, Misumi S, Okamoto Y, Otsuka M, Fujita M.** 2010. Highly sensitive analysis of the interaction between HIV-1 Gag and phosphoinositide derivatives based on surface plasmon resonance. Biochemistry **49:**5109–5116. http://dx.doi.org/10.1021/bi9019274.
14. **Chang CY, Chang YF, Wang SM, Tseng YT, Huang KJ, Wang CT.** 2008. HIV-1 matrix protein repositioning in nucleocapsid region fails to confer virus-like particle assembly. Virology **378:**97–104. http://dx.doi.org/10.1016/j.virol.2008.05.010.
15. **Cimarelli A, Luban J.** 1999. Translation elongation factor 1-alpha interacts specifically with the human immunodeficiency virus type 1 Gag polyprotein. J Virol **73:**5388–5401.
16. **Lochrie MA, Waugh S, Pratt DG, Jr, Clever J, Parslow TG, Polisky B.** 1997. In vitro selection of RNAs that bind to the human immunodeficiency virus type-1 gag polyprotein. Nucleic Acids Res **25:**2902–2910. http://dx.doi.org/10.1093/nar/25.14.2902.
17. **Purohit P, Dupont S, Stevenson M, Green MR.** 2001. Sequence-specific interaction between HIV-1 matrix protein and viral genomic RNA revealed by in vitro genetic selection. RNA **7:**576–584. http://dx.doi.org/10.1017/S1355838201002023.
18. **Chukkapalli V, Oh SJ, Ono A.** 2010. Opposing mechanisms involving RNA and lipids regulate HIV-1 Gag membrane binding through the highly basic region of the matrix domain. Proc Natl Acad Sci U S A **107:**1600–1605. http://dx.doi.org/10.1073/pnas.0908661107.
19. **Dick RA, Kamynina E, Vogt VM.** 2013. Effect of multimerization on

membrane association of Rous sarcoma virus and HIV-1 MA proteins. J Virol **87:**13598–13608. http://dx.doi.org/10.1128/JVI.01659-13.

20. **Inlora J, Chukkapalli V, Derse D, Ono A.** 2011. Gag localization and virus-like particle release mediated by the matrix domain of human T-lymphotropic virus type 1 Gag are less dependent on phosphatidylinositol-(4,5)-bisphosphate than those mediated by the matrix domain of HIV-1 Gag. J Virol **85:**3802–3810. http://dx.doi.org/10.1128/JVI.02383-10.
21. **Chukkapalli V, Inlora J, Todd GC, Ono A.** 2013. Evidence in support of RNA-mediated inhibition of phosphatidylserine-dependent HIV-1 Gag membrane binding in cells. J Virol **87:**7155–7159. http://dx.doi.org/10.1128/JVI.00075-13.
22. **Kutluay SB, Zang T, Blanco-Melo D, Powell C, Jannain D, Errando M, Bieniasz PD.** 2014. Global changes in the RNA binding specificity of HIV-1 gag regulate virion genesis. Cell **159:**1096–1109. http://dx.doi.org/10.1016/j.cell.2014.09.057.
23. **Alfadhli A, McNett H, Tsagli S, Bachinger HP, Peyton DH, Barklis E.** 2011. HIV-1 matrix protein binding to RNA. J Mol Biol **410:**653–666. http://dx.doi.org/10.1016/j.jmb.2011.04.063.
24. **Alfadhli A, Still A, Barklis E.** 2009. Analysis of human immunodeficiency virus type 1 matrix binding to membranes and Nucleic acids. J Virol **83:**12196–12203. http://dx.doi.org/10.1128/JVI.01197-09.
25. **Jones CP, Datta SA, Rein A, Rouzina I, Musier-Forsyth K.** 2011. Matrix domain modulates HIV-1 Gag's nucleic acid chaperone activity via inositol phosphate binding. J Virol **85:**1594–1603. http://dx.doi.org/10.1128/JVI.01809-10.
26. **Risselada HJ, Marrink SJ.** 2009. Curvature effects on lipid packing and dynamics in liposomes revealed by coarse grained molecular dynamics simulations. Phys Chem Chem Phys **11:**2056–2067. http://dx.doi.org/10.1039/b818782g.
27. **Kel O, Tamimi A, Fayer MD.** 2014. Size-dependent ultrafast structural dynamics inside phospholipid vesicle bilayers measured with 2D IR vibrational echoes. Proc Natl Acad Sci U S A **111:**918–923. http://dx.doi.org/10.1073/pnas.1323110111.
28. **Hogue IB, Hoppe A, Ono A.** 2009. Quantitative fluorescence resonance energy transfer microscopy analysis of the human immunodeficiency virus type 1 Gag-Gag interaction: relative contributions of the CA and NC domains and membrane binding. J Virol **83:**7322–7336. http://dx.doi.org/10.1128/JVI.02545-08.
29. **Diaz-Rohrer BB, Levental KR, Simons K, Levental I.** 2014. Membrane raft association is a determinant of plasma membrane localization. Proc Natl Acad Sci U S A **111:**8500–8505. http://dx.doi.org/10.1073/pnas.1404582111.
30. **Sezgin E, Kaiser HJ, Baumgart T, Schwille P, Simons K, Levental I.** 2012. Elucidating membrane structure and protein behavior using giant plasma membrane vesicles. Nat Protoc **7:**1042–1051. http://dx.doi.org/10.1038/nprot.2012.059.
31. **Carlton J, Bujny M, Peter BJ, Oorschot VM, Rutherford A, Mellor H, Klumperman J, McMahon HT, Cullen PJ.** 2004. Sorting nexin-1 mediates tubular endosome-to-TGN transport through coincidence sensing of high-curvature membranes and 3-phosphoinositides. Curr Biol **14:**1791–1800. http://dx.doi.org/10.1016/j.cub.2004.09.077.
32. **Gallop JL, Walrant A, Cantley LC, Kirschner MW.** 2013. Phosphoinositides and membrane curvature switch the mode of actin polymerization via selective recruitment of toca-1 and Snx9. Proc Natl Acad Sci U S A **110:**7193–7198. http://dx.doi.org/10.1073/pnas.1305286110.
33. **Hubner S, Couvillon AD, Kas JA, Bankaitis VA, Vegners R, Carpenter CL, Janmey PA.** 1998. Enhancement of phosphoinositide 3-kinase (PI 3-kinase) activity by membrane curvature and inositol-phospholipid-binding peptides. Eur J Biochem **258:**846–853. http://dx.doi.org/10.1046/j.1432-1327.1998.2580846.x.
34. **Yamauchi S, Fusada N, Hayashi H, Utsumi T, Uozumi N, Endo Y, Tozawa Y.** 2010. The consensus motif for N-myristoylation of plant proteins in a wheat germ cell-free translation system. FEBS J **277:**3596–3607. http://dx.doi.org/10.1111/j.1742-4658.2010.07768.x.
35. **Keller H, Krausslich HG, Schwille P.** 2013. Multimerizable HIV Gag derivative binds to the liquid-disordered phase in model membranes. Cell Microbiol **15:**237–247. http://dx.doi.org/10.1111/cmi.12064.
36. **Saleem M, Morlot S, Hohendahl A, Manzi J, Lenz M, Roux A.** 2015. A balance between membrane elasticity and polymerization energy sets the shape of spherical clathrin coats. Nat Commun **6:**6249. http://dx.doi.org/10.1038/ncomms7249.
37. **Carlson LA, Hurley JH.** 2012. In vitro reconstitution of the ordered assembly of the endosomal sorting complex required for transport at membrane-bound HIV-1 Gag clusters. Proc Natl Acad Sci U S A **109:**16928–16933. http://dx.doi.org/10.1073/pnas.1211759109.
38. **Lingappa JR, Reed JC, Tanaka M, Chutiraka K, Robinson BA.** 2014. How HIV-1 Gag assembles in cells: putting together pieces of the puzzle. Virus Res **193:**89–107. http://dx.doi.org/10.1016/j.virusres.2014.07.001.
39. **de Rocquigny H, El Meshri SE, Richert L, Didier P, Darlix JL, Mely Y.** 2014. Role of the nucleocapsid region in HIV-1 Gag assembly as investigated by quantitative fluorescence-based microscopy. Virus Res **193:**78–88. http://dx.doi.org/10.1016/j.virusres.2014.06.009.
40. **Mulet X, Rosivatz E, Ho KK, Gauthe BL, Ces O, Templer RH, Woscholski R.** 2009. Spatial localization of PtdInsP2 in phase-separated giant unilamellar vesicles with a fluorescent PLC-delta 1 PH domain. Methods Mol Biol **462:**135–144. http://dx.doi.org/10.1007/978-1-60327-115-8_8.
41. **Varnai P, Balla T.** 1998. Visualization of phosphoinositides that bind pleckstrin homology domains: calcium- and agonist-induced dynamic changes and relationship to myo-[^{3}H]inositol-labeled phosphoinositide pools. J Cell Biol **143:**501–510. http://dx.doi.org/10.1083/jcb.143.2.501.
42. **Casal HL, Mantsch HH, Demel RA, Paltauf F, Lipka G, hauser H.** 1990. Phase behavior and physical-chemical properties of N-methylated phosphatidylserine. J Am Chem Soc **112:**3887–3895. http://dx.doi.org/10.1021/ja00166a024.
43. **Pedersen TB, Sabra MC, Frokjaer S, Mouritsen OG, Jorgensen K.** 2001. Association of acylated cationic decapeptides with dipalmitoylphosphatidylserine-dipalmitoylphosphatidylcholine lipid membranes. Chem Phys Lipids **113:**83–95. http://dx.doi.org/10.1016/S0009-3084(01)00177-3.
44. **Sergelius C, Yamaguchi S, Yamamoto T, Engberg O, Katsumura S, Slotte JP.** 2013. Cholesterol's interactions with serine phospholipids - a comparison of N-palmitoyl ceramide phosphoserine with dipalmitoyl phosphatidylserine. Biochim Biophys Acta **1828:**785–791. http://dx.doi.org/10.1016/j.bbamem.2012.11.009.
45. **Stachowiak JC, Hayden CC, Sasaki DY.** 2010. Steric confinement of proteins on lipid membranes can drive curvature and tubulation. Proc Natl Acad Sci U S A **107:**7781–7786. http://dx.doi.org/10.1073/pnas.0913306107.
46. **Liposwsky R, Dimova R.** 2003. Domains in membranes and vesicles. J Phys Condensed Matter **15:**S31. http://dx.doi.org/10.1088/0953-8984/15/1/304.
47. **Baumgart T, Das S, Webb WW, Jenkins JT.** 2005. Membrane elasticity in giant vesicles with fluid phase coexistence. Biophys J **89:**1067–1080. http://dx.doi.org/10.1529/biophysj.104.049692.
48. **Bagatolli LA, Gratton E.** 2000. Two photon fluorescence microscopy of coexisting lipid domains in giant unilamellar vesicles of binary phospholipid mixtures. Biophys J **78:**290–305. http://dx.doi.org/10.1016/S0006-3495(00)76592-1.
49. **Korlach J, Schwille P, Webb WW, Feigenson GW.** 1999. Characterization of lipid bilayer phases by confocal microscopy and fluorescence correlation spectroscopy. Proc Natl Acad Sci U S A **96:**8461–8466. http://dx.doi.org/10.1073/pnas.96.15.8461.
50. **Lindwasser OW, Resh MD.** 2002. Myristoylation as a target for inhibiting HIV assembly: unsaturated fatty acids block viral budding. Proc Natl Acad Sci U S A **99:**13037–13042. http://dx.doi.org/10.1073/pnas.212409999.
51. **Charlier L, Louet M, Chaloin L, Fuchs P, Martinez J, Muriaux D, Favard C, Floquet N.** 2014. Coarse-grained simulations of the HIV-1 matrix protein anchoring: revisiting its assembly on membrane domains. Biophys J **106:**577–585. http://dx.doi.org/10.1016/j.bpj.2013.12.019.
52. **Redfern DA, Gericke A.** 2005. pH-dependent domain formation in phosphatidylinositol polyphosphate/phosphatidylcholine mixed vesicles. J Lipid Res **46:**504–515. http://dx.doi.org/10.1194/jlr.M400367-JLR200.
53. **Kooijman EE, King KE, Gangoda M, Gericke A.** 2009. Ionization properties of phosphatidylinositol polyphosphates in mixed model membranes. Biochemistry **48:**9360–9371. http://dx.doi.org/10.1021/bi9008616.
54. **Ellenbroek WG, Wang YH, Christian DA, Discher DE, Janmey PA, Liu AJ.** 2011. Divalent cation-dependent formation of electrostatic PIP2 clusters in lipid monolayers. Biophys J **101:**2178–2184. http://dx.doi.org/10.1016/j.bpj.2011.09.039.
55. **Casal HL, McElhaney RN.** 1990. Quantitative determination of hydrocarbon chain conformational order in bilayers of saturated phosphatidylcholines of various chain lengths by Fourier transform infrared spectroscopy. Biochemistry **29:**5423–5427. http://dx.doi.org/10.1021/bi00475a002.
56. **Chan R, Uchil PD, Jin J, Shui G, Ott DE, Mothes W, Wenk MR.** 2008.

Retroviruses human immunodeficiency virus and murine leukemia virus are enriched in phosphoinositides. J Virol **82:**11228–11238. http://dx.doi.org/10.1128/JVI.00981-08.

57. **Lorizate M, Sachsenheimer T, Glass B, Habermann A, Gerl MJ, Krausslich HG, Brugger B.** 2013. Comparative lipidomics analysis of HIV-1 particles and their producer cell membrane in different cell lines. Cell Microbiol **15:**292–304. http://dx.doi.org/10.1111/cmi.12101.
58. **Nguyen LN, Lim YS, Pham LV, Shin HY, Kim YS, Hwang SB.** 2014. Stearoyl coenzyme A desaturase 1 is associated with hepatitis C virus replication complex and regulates viral replication. J Virol **88:**12311–12325. http://dx.doi.org/10.1128/JVI.01678-14.
59. **Lyn RK, Singaravelu R, Kargman S, O'Hara S, Chan H, Oballa R, Huang Z, Jones DM, Ridsdale A, Russell RS, Partridge AW, Pezacki JP.** 2014. Stearoyl-CoA desaturase inhibition blocks formation of hepatitis C virus-induced specialized membranes. Sci Rep **4:**4549. http://dx.doi.org/10.1038/srep04549.